

## Electronic supplement for “Simple measures of ozone depletion in the polar stratosphere”

Rolf Müller<sup>1</sup>, Jens-Uwe Grooß<sup>1</sup>, Carsten Lemmen<sup>1,2</sup>, Daniel Heinze<sup>1</sup>, Martin Dameris<sup>3</sup>, and Greg Bodeker<sup>4</sup>

<sup>1</sup>ICG-1, Forschungszentrum Jülich, 52425 Jülich, Germany

<sup>2</sup>now at Copernicus Instituut voor Duurzame Ontwikkeling en Innovatie, Universiteit Utrecht, 3584CS Utrecht, The Netherlands and Institut für Küstenforschung, GKSS-Forschungszentrum Geesthacht GmbH, 21502 Geesthacht, Germany

<sup>3</sup>DLR, IPA, Oberpfaffenhofen, Germany

<sup>4</sup>NIWA, Private Bag 50061, Omakau Central Otago, New Zealand

The purpose of this electronic supplement is to provide additional information on the mean ozone over the polar cap, to discuss the location of the minimum ozone column and the maximum chemical ozone column loss relative to the location of the vortex edge in the E39/C model, and to provide a more detailed discussion of differences between between vortex size in models and in meteorological analyses.

In the main paper, the mean ozone over the polar cap was discussed extensively (see Figs. 1 and 2 of the main paper). Here we show in addition mean ozone over the polar cap for the Arctic in April (Fig. 1) and for the Antarctic in October (Fig. 2).

In the main paper, it was argued that for many years the minimum ozone is located outside the polar vortex in the presented E39/C timeslices. The erroneous association of the minimum column ozone with high chemical ozone loss becomes clear in a comparison with analysed chemical ozone loss. Chemical ozone loss based on a methane-ozone tracer correlation with the reference relation established on 1 January each simulated year and compared to the 1 April methane-ozone relation was first presented by Lemmen (2005) for this data set. Here, the loss values are recalculated based on an improved method for determining the vortex edge. The vortex edge was determined by fitting a third-order polynomial to the potential vorticity (PV) distribution as a function of  $\Phi_e$  for each potential temperature level between 340–640 K, defining the vortex edge by the steepest PV gradient constrained by the wind maximum on each level, converting the PV value at the vortex boundary to modified PV (Lait, 1994), and then using the median of these modified PV values as the criterion for distinguishing between vortex and out-of-vortex air masses in the model. The ozone column and vortex data for individual years of both time slice experiments are listed in separate files in the electronic supplement.

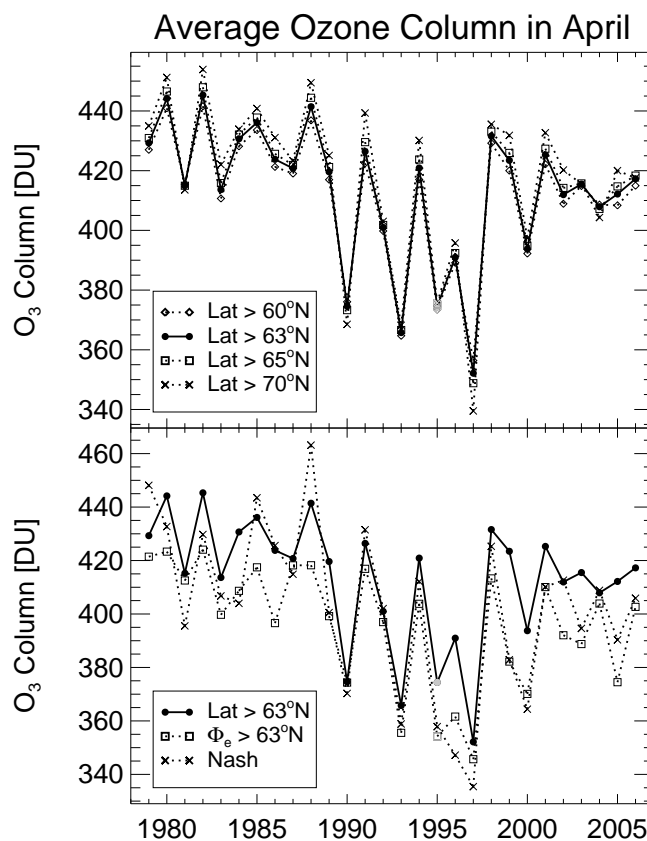


**Fig. 1.** Top panel: the April mean of Arctic ozone for a latitude boundary at 60°N, 63°N, 65°N, and 70°N. Bottom panel: the April mean of Arctic ozone for a latitude boundary at 63°N is compared with calculations using the equivalent latitude of 63°N and the maximum gradient in potential vorticity (applied on the 475 K potential temperature surface) as vortex edge definitions. All averages are area weighted averages.

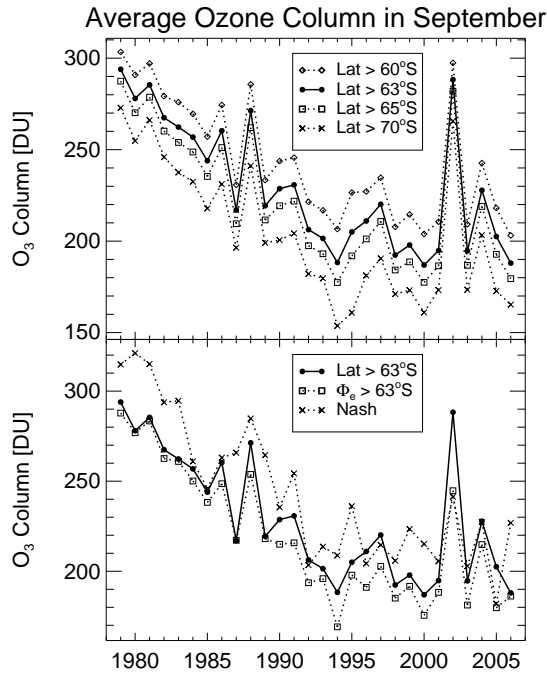


**Fig. 2.** Top panel: the September mean of Antarctic ozone for a latitude boundary at  $60^{\circ}\text{S}$ ,  $63^{\circ}\text{S}$ ,  $65^{\circ}\text{S}$ , and  $70^{\circ}\text{S}$ . Bottom panel: the September mean of Antarctic ozone for a latitude boundary at  $63^{\circ}\text{S}$  is compared with calculations using the equivalent latitude of  $63^{\circ}\text{S}$  and the Nash criterion (applied on the 475 K potential temperature surface) as vortex edge definitions.

For both time slices, Fig. 3 relates the location (in equivalent latitude) of the minimum ozone column and the maximum chemical ozone column loss to the location of the vortex edge as defined by Nash et al. (1996). For all winters of both time slice experiments, the maximum chemical column ozone loss is located within (or, in two cases, on) the polar vortex edge, i.e., in the shaded region in Fig. 3. For only three winters in each time slice experiment is the polar cap ozone minimum located within the vortex. On the ensemble average (determined separately for each time slice, uncertainty given as one standard deviation), the vortex edge is located at  $\Phi_e \approx 74^{\circ} \pm 8^{\circ}$  in 1990 ( $78^{\circ} \pm 6^{\circ}$  for ‘future’), and the location of the polar cap minimum is around  $62^{\circ} \pm 15^{\circ}$  ( $57^{\circ} \pm 13^{\circ}$ ), i.e., clearly outside of the vortex.

Further, we provide here additional information on the discussion of differences between between vortex size in models and in meteorological analyses. The fact that the size of the Arctic vortex in E39/C is smaller than in reality is discussed briefly in section 3.2.2 of the main paper. This fact is highlighted here in Fig. 4 where the strength of the barrier to meridional transport ( $\kappa = \nabla PV \cdot v$ , where  $v$  is the absolute value of the horizontal wind velocity, Bodeker et al. 2001) is compared with the same quantity calculated using output from the transient run with E39/C (Dameris et al., 2005) as a function of equivalent latitude on the 550 K surface. Ob-

served potential vorticity and wind fields on the 550 K surface were obtained every 6 hours from the NCEP/NCAR re-analysis database for these calculations. We focus on the first ten days of April to avoid too much sampling of vortex breakdowns which are more likely to occur towards the end of April and on the years 1990-1999 to focus on the period when ozone depletion over the Arctic is maximised.

Clearly the dynamical vortex in E39/C is weaker and broader than in reality and leans poleward. As a result, moving poleward in E39/C, ozone decreases more slowly than in reality. Furthermore, the dynamical vortex in the Arctic, as inferred from the maximum in  $\kappa$ , would be smaller in area in E39/C (at  $\Phi_e \approx 73^{\circ}$ ) than in reality (at  $\Phi_e \approx 69^{\circ}$ , Karpetchko et al., 2005). A similar result is reported by Tilmes et al. (2007) for the WACCM3 model, where the maximum of  $\kappa$  in the Arctic is smaller in magnitude and located further poleward with a much wider peak compared to observations.

Finally, We provide tabulated numbers for the values shown in several plots in the main paper for easier use. Listed in separate files are the ozone column and vortex data for individual years of the time slice experiments (shown in Fig. 3 in this supplement), the values for mean column ozone over the polar cap for the Arctic and for the Antarctic (see Figs. 1 and 2 of the main paper), the minimum of the daily average ozone in spring poleward of a threshold value (see Figs. 6 and 7 of the main paper). We also provide the values for  $V_{\text{PSC}}$  for the Arctic that are used in the paper and the PFP values employed here (which constitute a slightly updated version of the values presented earlier, Tilmes et al. 2006).

## References

- Bodeker, G. E., Scott, J. C., Kreher, K., and McKenzie, R. L.: Global ozone trends in potential vorticity coordinates using TOMS and GOME intercompared against the Dobson network: 1978-1998, *J. Geophys. Res.*, 106, 23 029–23 042, 2001.
- Dameris, M., Grewe, V., Ponater, M., Deckert, R., Eyring, V., Mager, F., Matthes, S., Schnadt, C., Stenke, A., Steil, B., Brühl, C., and Giorgetta, M. A.: Long-term changes and variability in a transient simulation with a chemistry-climate model employing realistic forcing, *Atmos. Chem. Phys.*, 5, 2121–2145, 2005.
- Karpetchko, A., Kyrö, E., and Knudsen, B. M.: Arctic and Antarctic polar vortices 1957-2002 as seen from the ERA-40 reanalyses, *J. Geophys. Res.*, 110, D21109, doi:10.1029/2005JD006113, 2005.
- Lait, L. R.: An alternative form for potential vorticity, *J. Atmos. Sci.*, 51, 1754–1759, 1994.
- Lemmen, C.: Future polar ozone: predictions of Arctic ozone recovery in a changing climate, Ph D thesis, Bergische Universität Wuppertal, 2005.
- Nash, E. R., Newman, P. A., Rosenfield, J. E., and Schoeberl, M. R.: An objective determination of the polar vortex using Ertel’s potential vorticity, *J. Geophys. Res.*, 101, 9471–9478, 1996.
- Tilmes, S., Müller, R., Engel, A., Rex, M., and Russell III, J.: Chemical ozone loss in the Arctic and Antarctic stratosphere

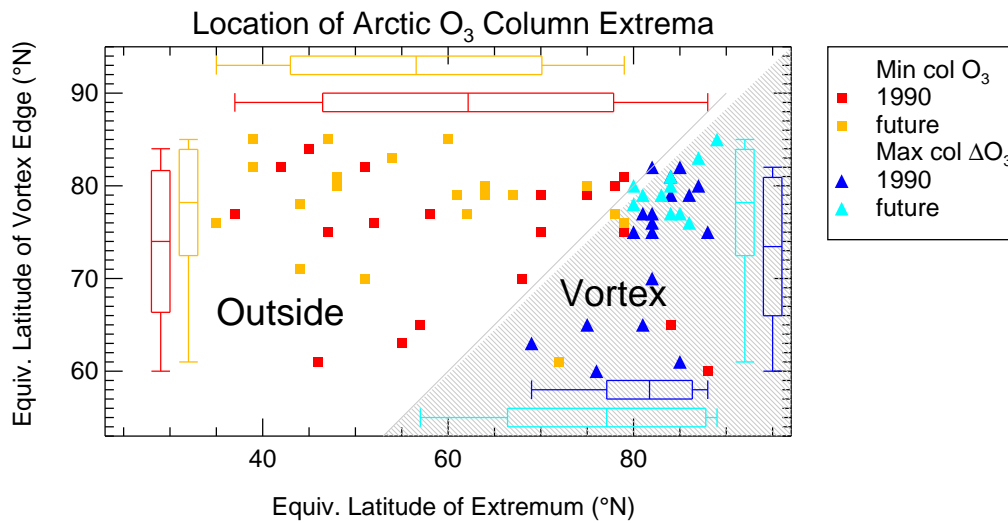


**Fig. 3.** Simulated 1 April location of the minimum ozone column and the maximum chemical loss column from two CCM 20-year ensemble (time slice) experiments with 1990 (blue, red) and near-future (dark yellow, cyan) boundary conditions for greenhouse gases and sea surface temperatures. For each time slice and for each analysis method (spatial minimum ozone column within the polar cap and spatial maximum of tracer-tracer correlation derived maximum chemical ozone loss). Box-whisker diagrams indicate the respective mean, standard deviation, and range of locations. The shaded area denotes the polar vortex.

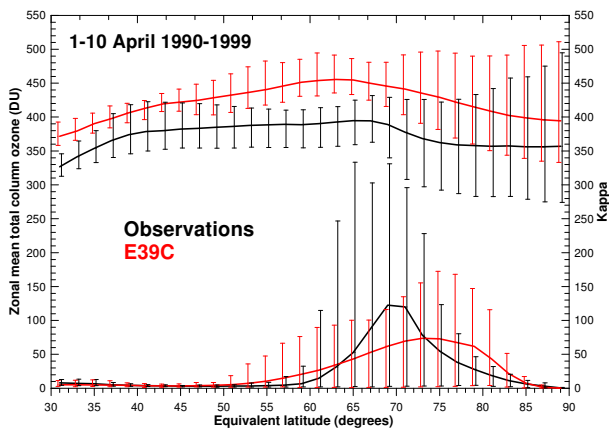


**Fig. 4.** Equivalent latitude (on the 550 K surface) zonal mean total column ozone (top two curves plotted against the left ordinate), and the strength of the barrier to meridional transport  $\kappa$ , (bottom two curves plotted against the right ordinate) for the northern hemisphere averaged over the years 1990–1999 and 1–10 April. Observations are shown in black and model results (from the transient run of E39/C, Dameris et al., 2005) in red. The vertical bars show the extremes (maximum and minimum values over the period).

between 1992 and 2005, *Geophys. Res. Lett.*, 33, L20812, doi: 10.1029/2006GL026925, 2006.

Tilmes, S., Kinnisen, D., Müller, R., Sassi, F., Marsh, D., Boville, B., and Garcia, R.: Evaluation of heterogeneous processes in the polar lower stratosphere in WACCM3, *J. Geophys. Res.*, doi:10.1029/2006JD008334, accepted, 2007.